Tumor suppressor SET9 guides the epigenetic plasticity of breast cancer cells and serves as an early-stage biomarker for predicting metastasis

MF. Montenegro[1], L Sánchez-del-Campo[2], R González-Guerrero[1], E Martínez-Barba[3], A Piñero-Madrona[4], J Cabezas-Herrera[5] and JN Rodríguez-López[1]

[1]Department of Biochemistry and Molecular Biology A, School of Biology, University of Murcia, Instituto Murciano de Investigación Biosanitaria (IMIB), Murcia, Spain. [2]Ludwig Institute for Cancer Research, Nuffield Department of Clinical Medicine, University of Oxford, Headington, Oxford, OX3 7DQ, UK. [3]Department of Pathology, University Hospital Virgen de la Arrixaca, IMIB, Murcia, Spain. [4]Department of Surgery, University Hospital Virgen de la Arrixaca, IMIB, Murcia, Spain. [5]Molecular Therapy and Biomarkers Research Group, University Hospital Virgen de la Arrixaca, IMIB, Murcia, Spain. Correspondence should be addressed to J.C-H. (juan.cabezas@carm.es) and J.N.R-L. (neptuno@um.es).

Running title: Epigenetic plasticity of breast tumors

CONFLICT OF INTEREST

The authors declare no competing financial interests.

Abstract

During the course of cancer progression, neoplastic cells undergo dynamic and reversible transitions between multiple phenotypic states, and this plasticity is enabled by underlying shifts in epigenetic regulation. Our results identified a negative feedback loop in which SET9 controls DNA methyltransferase-1 protein stability, which represses the transcriptional activity of the SET9 promoter in coordination with Snail. The modulation of SET9 expression in breast cancer cells revealed a connection with E2F1 and the silencing of SET9 was sufficient to complete an epigenetic program that favored epithelial-mesenchymal transition and the generation of cancer stem cells, indicating that SET9 plays a role in modulating breast cancer metastasis. SET9 expression levels were significantly higher in samples from patients with pathological complete remission than in samples from patients with disease recurrence, which indicates that SET9 acts as a tumor suppressor in breast cancer and that its expression may serve as a prognostic marker for malignancy.

Keywords: breast cancer; epigenetics; tumor suppressor; protein methylation; metastasis

INTRODUCTION

Cancer is an epigenetic disease to the degree that it can be considered a genetic disease[1]. Epigenetic profiles are susceptible to change and thus can help explain how certain environmental factors may increase the risk of cancer[2]. Unlike the static nature of the gene sequence, the dynamic nature of epigenetic regulation provides a mechanism for reprogramming gene function in response to cancer therapies. Thus, identifying epigenetic changes that are associated with the development and progression of cancers might have important implications for human health, because they are potentially reversible and amenable to therapeutic intervention[3]. Once we understand the factors that modify these epigenetic processes, we might also be able to design therapeutic strategies to revert adverse epigenetic phenotypes. In addition to methylation of DNA and histones, methylation of non-histone proteins, such as transcription factors, is also implicated in the biology and development of cancer[4]. Among the methyltransferases, SET9 (also known as SETD7) plays a prominent role in lysine methylation of histones and non-histone proteins and its activity has been associated with loss of DNA methylation[5], chromatin remodeling[6], and regulation of transcription factors such as p53, estrogen receptor α (ERα), and E2F1, among others[7-10]. Thus, by combining these catalytic functions, SET9 could constitute a fine-tuning mechanism for the epigenetic modulation of gene expression. E2F1 and its pro-apoptotic genes represent such a group of molecules and hence have direct implications as targets for anti-neoplastic therapeutics for cancer lacking p53 activity. Although first recognized as a key regulator of apoptosis, recent evidence has revealed that E2F1 expression is aberrantly high in late-stage cancers and promotes tumor invasion and metastasis instead of apoptosis[11]. Due to its oncogenic nature, E2F1 has also been implicated in the mechanisms of resistance of cancer cells to chemotherapy and radiotherapy, facilitation of DNA repair and inhibition of senescence induction[12-15]. Since SET9 controls the posttranslational modifications of E2F1, SET9

regulation could be used as a tool to modulate E2F1 activity to favor its tumor suppressor function. Therefore, the aim of this study was to analyze the global consequences of DNA methyltransferase 1 (DNMT1) and E2F1 methylation by SET9 and its impact on the physiopathology of breast cancer (BC), and to explore the clinical utility of SET9 as a potential prognostic marker for BC malignancy.

RESULTS

A negative feedback loop between SET9 and DNMT1 determines the epigenetic phenotype of BC cells

In agreement with previous observations that methylation of DNMT1 by SET9 at Lys142 targeted DNMT1 protein for degradation by the proteasome[5], we observed an inverse relationship between the abundance of SET9 (at both mRNA and protein levels) and DNMT1 protein (Figure 1a) in BC cell lines. To generalize this observation, we investigated the relationship between SET9 and DNMT1 in a small cohort of clinical samples (n = 36) obtained from BC biopsies (Figure 1b). In general, high levels of SET9 mRNA corresponded to high levels of SET9 protein as well as low levels of DNMT1 protein. As previously observed in other cellular systems[5], overexpression or depletion of SET9 in MDA-MB-231 or MCF7 cells, respectively, had an opposite effect on DNMT1 protein abundance, but not on DNMT1 mRNA levels (Figure 1c,d), which clearly indicated that SET9 was critical to control DNMT1 protein stability. Since SET9 controlled DNMT1 at its protein level, we next investigated whether DNMT1 protein could reciprocally regulate SET9 expression. Silencing of DNMT1 or inhibition of its catalytic activity with 5-aza-deoxycytidine (5-Aza-dC) had a profound and positive effect on the activation of SET9 in MDA-MB-231 cells (Figure 1e), which indicated that DNMT1 controls the expression of SET9 by methylation of its gene promoter (see below). Therefore, these data reveal a negative feedback loop between SET9 and DNMT1 that determines the epigenetic phenotype of BC cells.

SET9 contributes to the epigenetic regulation of epithelial-mesenchymal transition

Aberrant DNA methylation has been involved in the enhancement of invasion and metastasis in cancer cells[16,17]. Overexpression of SET9 in MDA-MB-231 cells, a high metastatic cell line, resulted in mesenchymal-epithelial transition (MET) with upregulation of E-cadherin and a significant downregulation of both vimentin and EGFR expression (Figure 2a, Supplementary Figure 1a,b). In agreement with these expression patterns, overexpression of SET9 in MDA-MB-231 cells greatly inhibited the migratory ability of this cell line (Figure 2a). In contrast, silencing of SET9 in MCF7 cells (a low metastatic cell line) highly increased epithelial-mesenchymal transition (EMT) markers, disrupted cell-cell adhesion, and promoted invasiveness (Figure 2b, Supplementary Figure 1a,b,c). In addition to its control of protein stability, SET9 has also been involved in chromatin remodeling. SET-mediated methylation of H3-K4 functions in transcription activation by competing with histone deacetylases and by precluding H3-K9 methylation by Suv39h1[6], a methylase that together with Snail and DNMT1 is involved in E-cadherin repression[18,19]. Our results support this notion, since we observed that knockdown of SET9 expression in MCF7 cells favored H3K9 versus H3K4 methylation at the E-cadherin promoter (Figure 2c). The observations that silencing of SET9 in MCF7 cells significantly increased the nuclear localization of Snail (Supplementary Figure 1c), as well as its occupancy, together with DNMT1, on the E-cadherin promoter (Figure 2d) clearly support our hypothesis that SET9 is an important factor controlling EMT and BC metastasis.

Snail cooperates with DNMT1 to repress SET9 expression

Transient silencing of SET9 resulted in a stable SET9^{low} phenotype in MCF7 cells, which was maintained for indefinite cell passages (Supplementary Figure 2a). After cell injection in nude mice MCF7 cells transiently transfected with SET9 siRNAs were highly metastatic *in vivo* compared with the parental MCF7 cell line (Supplementary Figure 2b), which suggested that

lack of SET9 expression might be sufficient to activate an epigenetic program that blocks differentiation and favors EMT phenotypic conversion in BC cells. TNF-α induces the activation of EGFR signaling in human cancer cells and results in Snail transactivation[20] and we observed that TNF-α treatment was also accompanied by a strong repression of SET9 expression in MCF7 cells (Supplementary Figure 1d). Inspection of the 1.0 kb genomic DNA sequence upstream of the SET9 transcription initiation site revealed at least two potential Snail-binding consensus sites (E-box1: CAGGTG at position -610 to -605, and E-box2: CACCTG at -142 to -137). Therefore, we performed a ChIP assay to investigate the interaction between Snail and DNMT1 at the SET9 promoter *in vivo* (Figure 2e). Silencing of SET9 or TNF-α treatment highly increased the occupancy of Snail and DNMT1 in the SET9 promoter in MCF7 cells compared with controls. As predicted by these results, we found that both knockdown of SET9 or TNF-α treatment also resulted in an increase of SET9 promoter methylation (Figure 2e). These results, together with the reciprocal interplay between H3K4me2/3 and H3K9me3 in the SET9 promoter in control and siSET9-MCF7 cells (Figure 2c), suggested a similar mechanism for E-cadherin and SET9 repression during activation of the EMT program and supported an epigenetic mechanism by which microenvironmental signaling might favor SET9 repression and cancer metastasis.

SET9 and E2F1 are reciprocally regulated in BC cells

As with DNMT1, E2F1 has also been identified as a substrate of SET9[9,10]; however, there is currently no consensus on the impact of methylated Lys185 in E2F1. To answer this question, we studied the relationship between SET9 expression and E2F1 stability in BC cells and patient tissues (Figure 3a, Supplementary Figure 3a). Similar to the data obtained for DNMT1, we observed an inverse correlation between the abundance of SET9 and E2F1. Again, manipulation of cellular SET9 levels by silencing or promoting its expression in MCF7 or MDA-MB-231 cells, respectively, showed opposing effects on E2F1 protein

abundance (Figure 3b, Supplementary Figure 3b). Because real-time PCR in control and siSET9-MCF7 cells showed no difference in E2F1 mRNA levels (Supplementary Figure 3b), the higher abundance of E2F1 protein in siSET9-MCF7 cells than in the parental cells seems to be related to protein stabilization. Overexpressed E2F1-(K185L) mutant had higher protein stability than the overexpressed E2F1-(WT) in MCF7 cells (Figure 3c, Supplementary Figure 3c) and assays in the presence of MG132, a proteasome inhibitor (Supplementary Figure 3d), also confirmed the hypothesis that, at least in BC cells, E2F1 protein is dynamically modulated by methylation at Lys185 and that methylated E2F1 is the substrate for ubiquitylation[9].

We observed downregulation of SET9 and activation of EMT in MCF7 cells after overexpression of E2F1-(WT) that was further enhanced by stabilization of the E2F1-(K185L) mutant (Figure 3c, Supplementary Figure 3c,e). Consequently, accumulation of this transcription factor significantly enhanced EGFR and Snail expression, leading to the nuclear transactivation of Snail and the enrichment of this protein in the promoter of both SET9 and E-cadherin (Figure 3c, Supplementary Figure 3e). These results clearly indicated that E2F1 accumulation could indirectly regulate SET9 promoter activity. Therefore, we next investigated the effects of depleting E2F1 in MDA-MB-231 on the (R)-PFI2-induced activation of EMT in MCF7 cells. The growth rates of MDA-MB-231 cells expressing E2F1 siRNA or control siRNA were similar, indicating that E2F1 was not required for the proliferation of this metastatic cell line. Silencing E2F1 in MDA-MB-231 increased luminal markers, such as E-cadherin, while diminishing EGFR, a basal marker (Figure 3d), implicating this transcription factor in BC cell metastatic phenotypes. In agreement with previous results, the loss of E2F1 also resulted in a significant increase in SET9 and a decrease in both protein and mRNA levels of Snail. Consequently, silencing E2F1 resulted in a significant decrease in the Snail occupancy on both SET9 and E-cadherin promoters (Figure

3d). On the other hand, we observed that treating MCF7 cells with (R)-PFI2, a potent and selective inhibitor of SET9[21], stabilized E2F1 and resulted in EMT. However, the (R)-PFI2-dependent effects were not observed in the corresponding E2F1-silenced cells (Supplementary Figure 3f).

Altogether, the results indicated that E2F1 was necessary to repress SET9 activity and to induce EMT in BC cells; thus, by controlling Snail expression and transactivation, E2F1 may compensate for the tumor suppressor function of SET9. In addition, we also observed that by modulating the oncogenic activity of CIP2A, the SET9/E2F1 axis regulated the resistance or sensitivity of BC cells to senescence after DNA damage (Supplementary Figure 4)[14,15.] Therefore, SET9 levels in BC cells might be a good indication of the differentiation state of the cells and the susceptibility of these cells to different cancer therapies.

Loss of SET9 activity acts as a molecular link between EMT and the generation of cells with stem cell-like properties

Silencing of SET9 induced a durable CSC-like $CD44^{+}/CD24^{-/low}$ phenotype in MCF7 cells (Supplementary Figure 2a). Moreover, we noted that cells from MCF7 mammospheres showed a lower SET9 content than adherent cells (Supplementary Figure 5a), which seems to indicate that mammospheres could derived from an MCF7 population with a $SET9^{low}$ phenotype. To test this possibility, we analyzed whether silencing or overexpressing SET9 could affect the ability of MCF7 cells to form primary mammospheres (Figure 4a). In addition to increasing MCF7 mammosphere-forming capacity, silencing SET9 also accelerated mammosphere dedifferentiation[22]. Primary mammosphere cultures derived from siSET9-MCF7 cells completed EMT transformation in several days without needing additional cell reseeding or stem cell-inducing growth factors (Figure 4b). The reduction in cell–cell adhesion in these dedifferentiated mammospheres was paralleled by a marked decrease in E-cadherin expression and increased SOX2 (Sex-determining region Y (SRY)-

Box2) protein expression[23]. Silencing SET9 in MCF7 cells promoted a transient $CD44^{high}/CD24^{high}$ cell population, while siSET9-MCF7 dedifferentiated mammosphere-derived cells displayed a stable mesenchymal and CSC-like $CD44^{+}/CD24^{-/low}$ phenotype[24] (Figure 4c, Supplementary Figure 5b). As expected, overexpression of SET9 in MDA-MB-231 affected primary mammospheres differentiation in an opposite way enhancing E-cadherin expression and favoring cell aggregation (Supplementary Figure 5c). In addition, we also analyzed the effect of SET9 expression on secondary mammosphere formation to evaluate the role of this protein in self-renewal (Supplementary Figure 5d).

Next, we analyzed the expression of 84 genes related to identification, growth and differentiation of CSCs in primary mammospheres (Figure 4d, Supplementary Figure 6). When compared with the parental MCF7 cell line, SET9 silencing resulted in significant upregulation ($P < 0.05$; > 2-fold expression) of 30 genes, while only 4 genes (including *CDH1* or E-cadherin) were significantly downregulated. Interestingly, the results indicated that the expression of 24 upregulated genes after SET9 silencing was also significantly increased in MDA-MB-231 cells when compared with resting MCF7 cells. MDA-MB-231 differentiated mammospheres overexpressing SET9 showed a gene signature different from parental MDA-MB-231 cells, with upregulated E-cadherin and the downregulation of several genes related with stemness[25,26] (Figure 4d, Supplementary Figure 6).

SET9 as an early prognostic marker for BC malignancy

Although lymph node (LN) metastasis is still considered the most significant prognostic factor for BC outcome[27], this variable clearly depended on the time at which the cancer was diagnosed. Early detection of BC requires the identification of new biomarkers, which in initial stages of the disease could be predictive of malignancy and/or clinical outcomes of treatment regimens. To assess the validity of SET9 as a prognostic marker, we studied its expression in a cohort of breast tumor samples ($n = 87$). SET9 mRNA expression levels were

significantly higher in samples from patients harboring benign tumors or in those that showed pathological complete remission (pCR) than in samples from patients suffering of disease recurrence (Non-pCR) (Figure 5a, Supplementary Table S1). Combined Kaplan-Meier analysis of overall survival (OS) and disease free survival (DFS) using SET9 tumor status, under the cutoff value determined by receiver operating characteristic (ROC) curve analysis (Figure 5a), indicated that both OS and DFS declined significantly in patients with low SET9 expression (Figure 5b,c). As shown in Supplementary Table S2, differences in SET9 mRNA expression only correlated with IHC-quantified levels of Ki67, whereas with other factors, such as tumor size, LN, and ERα status, showed no correlation. To check the validity of SET9 expression as an early prognostic marker, we next compared SET9 expression in patients classified according to their initial staging (based on tumor grade, size and LN status) and their clinical response (pCR *vs*. Non-pCR) (Supplementary Table S1). Interestingly, SET9 mRNA expression in tumor biopsies correlated with the clinical outcome of BC patients independent of their primary staging and the administrated therapy (Supplementary Figure 7a). Of clinical relevance is the relationship found between SET9 mRNA status and the response to hormonal therapy in ERα-positive patients ($P < 0.001$; Figure 6d, Supplementary Figure 7b), indicating that SET9 levels could be used as a predictive marker for the resistance of tumors to anti-estrogenic therapies. Thus, SET9 expression may provide another specific definition of BC subtypes that better predicts patient survival. Finally, we used IHC to detect SET9 protein expression in FFPE samples (Figure 5e). When we used SET9 intensity in IHC samples (CRIF) to divide the 77 cases into two groups, we observed that low SET9 staining was associated with further distant spread. We used ROC curve analysis to calculate the optimal cutoff value to classify SET9 expression for predicting distant metastasis (Figure 5f). The area under the ROC curve (AUC) for SET9 expression was 0.872 ($P < 0.001$; 95%

confidence interval, 0.784–0.961), indicating that the baseline SET9 level based on a core biopsy specimen could be a very useful marker to predict BC metastasis.

DISCUSSION

The activation of EMT has been found to generate cells that either exhibit stem-like properties or are poised to enter into the stem cell state[3,28-32]. This acquisition of stem-like characteristics holds important implications for the successful completion of the invasion-metastasis cascade by disseminated cancer cells[31]. We observed that a negative feedback loop between SET9 and DNMT1 plays a predominant role in the epigenetic control of cell plasticity and this work identifies SET9 as a key determinant mediating properties shared by CSCs and EMT in BC tumors. Since SET9 controls the stability of DNMT1 protein, and this, in turn, in coordination with Snail, represses the transcriptional activity of the SET9 promoter, this negative feedback loop can efficiently maintain the mesenchymal phenotype of BC cells in the absence of continuous paracrine EMT-inducing signals[3,33]. Loss of SET9 activity also had a profound impact on chromatin epigenetics, favoring a histone modification pattern assigned to mesenchymal cell signature[3,34]. In addition, microenvironment signaling favoring SET9 repression may also increase E2F1 stability. Recent studies have shown that this transcription factor is relevant for cancer progression and tumor resistance; thus, increased abundance of E2F1 triggers invasion and metastasis by upregulating EGFR and activating the cytoplasmic Ras/mitogen-activated protein kinase (MAPK)/extracellular signal-regulated kinase (ERK) and PI3K/AKT signaling cascades[35,36]. EGFR is known to cooperate with E2F1 to induce B-Myb gene expression[37], and increased B-Myb upregulates Snail expression to promote EMT and invasion of BC cells[38]. Our results indicate that by controlling E2F1 stability, SET9 may avoid EMT and metastasis that is mediated by E2F1 in BC cells.

Multiple studies have shown that the aggregation of tumor cells is an important step not only in the dissemination of tumor cells from a tumor mass, but also in establishing metastatic

foci[39,40]. Opposed to the traditional interpretation of the metastatic process that considers that highly metastatic tumor cells lose the capacity for homotypic adherence, especially as a result of the loss or dysfunction of adherent molecules such as E-cadherin[41], an alternative explanation of metastatic dissemination has been proposed based on clinical and experimental observations[42]. According to this hypothesis, the aggregates of tumor cells are formed *in situ*, and the clumps spread through lymph fluid or the bloodstream forming tumor microemboli in distant microvessels[40]. During the EMT program guided by SET9 depletion, MCF7 cells transited on a spectrum of states that culminate in a CSC-like phenotype displaying $CD44^{+}/CD24^{-/low}$ markers; however, during the first steps of this EMT process, the cells resided on a highly differentiated basal/epithelial phenotype ($CD44^{high}/CD24^{high}$) with a marker expression of E-cadherin. A phenotype that promotes tumor cells aggregation while maintaining its metastatic capacity[43-45] might have competitive advantages for cell spreading during the metastatic process; aggregated cells could evade apoptosis triggered by loss of cell attachment (anoikis), escape from recognition by the immune system, and/or promote heterotypic interactions with inflamed endothelium[46]. The sequence of phenotypic changes induced for SET9 depletion identifies this protein as an important epigenetic factor favoring the homotypic aggregation of tumor cells during the EMT program. Therefore, drugs or treatments targeting the process of cell aggregation might result in prevention of CSC formation and metastasis.

This work also identified SET9 as a tumor suppressor protein in BC cells and accordingly, overexpression of its counterpart, lysine-specific demethylase 1 (LSD1), has been correlated with poor survival in several types of cancers[47,48]. In BC, LSD1 inhibition or destabilization conferred cell growth inhibition, suppression of CSCs *in vitro* and inhibition of tumorigenicity *in vivo*[49,50]. Analysis of SET9 mRNA and protein in BC tumors from a limited

cohort of patients suggested that its expression could be clinically useful as a potential prognostic marker for BC malignancy; however, larger confirmatory studies are required.

In conclusion, we observed that SET9 was necessary to maintain a luminal phenotype in BC cells, while its depletion resulted in EMT and acquiring a basal phenotype. Altogether, the results indicated that SET9 acts a tumor suppressor in BC cells by preventing aberrant accumulation of E2F1 and DNMT1 (Figure 6). Accumulation of E2F1 can compensate the tumor suppressor function of SET9, and it was recently observed that inhibition of DNMT1 induced anoikis and suppression of mammosphere formation in human breast cancer cells[51]. We report that SET9 and E-cadherin are repressed by a common mechanism, which indicates that SET9 repression may parallel E-cadherin repression during EMT (Figure 6). SET9 controls DNMT1 protein stability, which in turn represses the transcriptional activity of the SET9 promoter through coordination with Snail. This negative feedback loop efficiently maintains the mesenchymal phenotype of BC cells, including E-cadherin repression, in the absence of continuous paracrine EMT-inducing signals. Furthermore, these results may have therapeutic implications. Therapies designed to target the dynamic epigenetic machinery of BC cells[4,52], alone or in combination with DNA damage therapies, may be of clinical utility to induce apoptosis or senescence in refractory breast cancers and suppress CSC formation and cancer metastasis. Therefore, we believe that the phenotypic plasticity described here can open new avenues for the diagnostics and evasive breast tumor therapies.

MATERIALS AND METHODS

Patient-derived breast cancers.

The patient-derived BC samples are summarized in Supplementary Table S1. Fresh tumor samples were obtained from patients undergoing surgery for invasive ductal or lobular carcinomas (n = 77) and women with benign tumors (n = 10) and were used for mRNA and protein extraction. Fresh specimens were divided into sections and stored at -80ºC until use. Three randomly chosen slices from each tumor were used in phenol-chloroform-mediated total RNA extraction, and 3 other slices were used in protein extraction, as described below. Protein extracts were pooled and used in western blot analysis. RNA (5 µg) was used to synthetize cDNA, and equal amounts of the three cDNA fractions corresponding to the same tumor were pooled and used for real time RT-PCR quantifications of SET9 mRNA (see below). Formalin-fixed, paraffin-embedded, patient-derived tumors were used for immunohistochemistry (IHC) analyses (see below). Major pathological parameters were all available, including the tumor size, histological type, LN status, and pathological state according to the American Joint Committee on Cancer[53]. The statuses of ERα and Ki67 were determined by conventional IHC. Information on adjuvant treatments (chemotherapy, radiotherapy, and endocrine therapy) was obtained from the medical records of each patient. All patients were on regular follow-up schedules ranging from 12 to 162 months in duration with a mean follow-up of 87.05 months.

Cell cultures and treatments

The MCF-7 and MDA-MB-231 human BC cell lines were purchased from the American Type Culture Collection (ATCC), and they were routinely authenticated by genotype profiling, according to ATCC guidelines. Cells were routinely tested for mycoplasma contamination using MycoSET™ Mycoplasma Real-Time PCR detection Kit (Life Technologies, Foster City, CA). Cells were maintained in the appropriate culture medium

supplemented with 10% fetal bovine serum (FBS) and antibiotics. Cell viability was evaluated by a colorimetric assay for mitochondrial function using the 2,3-Bis(2-methoxy-4-nitro-5-sulfophenyl)-2H-tetrazolium-5-carboxanilide (XTT; Sigma) cell proliferation assay. For this assay, cells were plated in a 96-well plate at a density of 1000-2000 cells/well. For IR treatments, cells were irradiated with an Andrex SMART 200E machine (YXLON International, Hamburg, Germany) operating at 200 kV and 4.5 mA with a focus-object distance of 20 cm at room temperature and at dose rate of 2.5 Gy per min. The radiation doses were monitored by a UNIDOS® universal dosimeter with PTW Farme® ionization chamber TW 30010 (PTW-Freiburg, Freiburg, Germany) in the radiation cabin. Immediately after irradiation, cells were returned to the incubator for recovery until the appropriate time point.

Mammosphere culture conditions

Mammospheres were cultured in 24-well ultra-low-attachment plates (Corning Inc., Lowell, MA). Before plating, primary mammosphere cell suspensions were dissociated by incubating them for 2 min at 37ºC in 0.05% trypsin/EDTA followed by mechanical dissociation using a 22-gauge needle. The cells were then passed through a 40-µm sieve to obtain a single-cell suspension. Single cells were then plated at 500 cells/cm^2 to avoid cell-cell adhesion and secondary mammosphere formation assays were performed in serum-free stem cell medium containing DMEM/F12 (1:1) supplemented with B27 (GIBCO), 20 ng/ml EGF (Sigma), 10 ng/ml fibroblast growth factor (Sigma), and an antibiotic-anti-mycotic. For mammosphere dedifferentiation assays, adherent cells were trypsinized and plated at 10,000 cells/cm^2 in ultra-low-attachment plates. Complete primary mammospheres were cultured in the same culture mediums used for adherent cells to avoid the extra signaling that can be produced by specific growth factors that are enriched in standard stem cell medium. Mammosphere-forming efficiency (MFE) was calculated by dividing the number of mammospheres (colonies

> 50 μm in diameter) that were formed by the number of cells that were plated and then expressed as a percentage[54]. Each experiment was performed in triplicate.

Athymic *nu/nu* mice

Animals were bred and maintained according to the Spanish legislation on the 'Protection of Animals used for Experimental and other Scientific Purposes' and in accordance with the directives of the European Community. Female athymic *nu/nu* mice, 4–5 weeks of age (5 mice per group), were obtained from Harlan Laboratories (Indianapolis, IN). They were exposed to a 12-hr light/12-hr dark cycle, and had free access to a Harlan Teklad Rodent Diet 8604 (Harlan Teklad, Madison, WI) and water. Mice were housed under aseptic conditions (positive air pressure in a designated mouse room with microisolator tops), and all mouse-handling procedures were carried out under a laminar flow hood. After approximately two weeks of acclimatization after arrival, siCN-MCF7 or siSET9-MCF7 cells (5×10^6 cells in 100 μL PBS) containing a luciferase reporter were subcutaneously injected into the left flank of each animal. Primary tumors and metastases at 3 and 6 weeks were analyzed using the IVIS Imaging System (Caliper Life Sciences, Hopkinton, MA). We tried to reach the conclusion using as small a size of samples as possible. We usually excluded samples if we observed any abnormality in terms of size, weight or apparent disease symptoms in mice before performing experiments. However, we did not exclude animals here, as we did not observe any abnormalities in the present study. Neither randomization nor blinding was done in this study.

Statistical analysis

Western blotting and microscopy were repeated at least three times, and similar results were obtained. The results from one experiment are shown. For other experiments, the mean ± SD for 3 determinations in triplicate were calculated. We estimated the sample size considering

the variation and mean of the samples. Individual comparisons were made with Student's two-tailed, unpaired t-tests. Differences in SET9 expression were assessed using Chi-square tests. Numeric data were analyzed for statistical significance using Mann-Whitney tests. Kaplan-Meier curves were constructed to assess disease-free (DFS) or overall (OS) survival. The starting point for survival studies was the date of the surgical act, and the final point was the manifestation of either local recurrence, distant metastasis dissemination (DFS) or death (OS). If without recurrence, patients were censored on the last follow-up. Differences between groups were analyzed using the log-rank test for equality of survivor. The criterion for significance was $P < 0.05$ for all comparisons. Statistical tests are justified as appropriate for every figure, and the data meet the assumptions of the tests. Data were analyzed using the SPPS statistical software for Microsoft Windows version 15.0 (SPSS Inc., Chicago, IL).

Ethical Approval

Human tumor samples were collected from patients attending the Breast Unit in the Department of Surgery at the Hospital Universitario Virgen de la Arrixaca, Murcia, and from the Biobank at the Hospital General Universitario de Alicante (Red Valenciana de Biobancos y Red Nacional de Biobancos). Study approval and consent procedures were obtained from the Institutional Ethic Committees of Hospitals. All patients gave their consent after being appropriately informed. Animal procedures were approved by the Ethical Committee of the University of Murcia and the Direccion General de Ganaderia y Pesca, Comunidad Autonoma de Murcia (Project reference A1320140710).

ACKNOWLEDGEMENTS

This work was supported by grants from Ministerio de Economia y Competitividad (MINECO; Co-financing with Fondos FEDER) (SAF2013-48375-C2-1-R) to J.N.R-L and Fundación Séneca, Región de Murcia (FS-RM) (15230/PI/10 and 19304/PI/14) to J.N.R-L, J.C-H, and A.P-M. J.C-H is contracted by the FFIS. M.F.M is contracted by Fundación de la Asociación Española contra el Cáncer (FAECC). L.S-d-C is supported by the Ludwig Institute for Cancer Research and FAECC.

Supplementary Information accompanies the paper on the Oncogene website (http://www.nature.com/onc)

REFERENCES

1. Esteller M, Herman JG. Cancer as an epigenetic disease: DNA methylation and chromatin alterations in human tumours. J Pathol 2002;196:1-7.
2. Esteller M. Aberrant DNA methylation as a cancer-inducing mechanism. Annu Rev Pharmacol Toxicol 2005;45:629-656.
3. Tam WL, Weinberg RA. The epigenetics of epithelial-mesenchymal plasticity in cancer. Nat Med 2013;19:1438-49.
4. Montenegro MF, Sánchez-del-Campo L, Fernández-Pérez MP, Sáez-Ayala M, Cabezas-Herrera J, Rodríguez-López JN. Targeting the epigenetic machinery of cancer cells. Oncogene 2014; 34:135-143.
5. Estève PO, Chin HG, Benner J, Feehery GR, Samaranayake M, Horwitz GA, *et al*. Regulation of DNMT1 stability through SET7-mediated lysine methylation in mammalian cells. Proc Natl Acad Sci USA 2009;106:5076-5081.
6. Nishioka K, Chuikov S, Sarma K, Erdjument-Bromage H, Allis CD, Tempst P, *et al*. Set9, a novel histone H3 methyltransferase that facilitates transcription by precluding histone tail modifications required for heterochromatin formation. Genes Dev 2002;16:479-489.
7. Chuikov S, Kurash JK, Wilson JR, Xiao B, Justin N, Ivanov GS, *et al.* Regulation of p53 activity through lysine methylation. Nature 2004;432:353-60.
8. Subramanian K, Jia D, Kapoor-Vazirani P, Powell DR, Collins RE, Sharma D, *et al.* Regulation of estrogen receptor alpha by the SET7 lysine methyltransferase. Mol Cell 2008;30:336-347.
9. Kontaki H, Talianidis I. Lysine methylation regulates E2F1-induced cell death. Mol Cell 2010;39:152–160.

10. Xie Q, Bai Y, Wu J, Sun Y, Wang Y, Zhang Y *et al.* Methylation-mediated regulation of E2F1 in DNA damage-induced cell death. J Recept Signal Transduct Res 2011;31:139-146.
11. Alla V, Engelmann D, Niemetz A, Pahnke J, Schmidt A, Kunz M, *et al.* E2F1 in melanoma progression and metastasis. J Natl Cancer Inst 2010;102:127-133.
12. Biswas AK, Johnson DG. Transcriptional and nontranscriptional functions of E2F1 in response to DNA damage. Cancer Res 2012;72:13-17.
13. Pützer BM, Engelmann D. E2F1 apoptosis counterattacked: evil strikes back. Trends Mol Med 2013;19:89-98.
14. Laine A, Sihto H, Come C, Rosenfeldt MT, Zwolinska A, Niemelä M, *et al.* Senescence sensitivity of breast cancer cells is defined by positive feedback loop between CIP2A and E2F1. Cancer Discov 2013;3:182-197.
15. Laine A, Westermarck J. Molecular pathways: Harnessing E2F1 regulation for prosenescence therapy in p53-defective cancer cells. Clin Cancer Res 2014; 20:3644-3650.
16. Wang JF, Dai DQ. Metastatic suppressor genes inactivated by aberrant methylation in gastric cancer. World J Gastroenterol 2007; 13:5692-5698.
17. Montenegro MF, Sáez-Ayala M, Piñero-Madrona A, Cabezas-Herrera J, Rodríguez-López JN. Reactivation of the tumour suppressor RASSF1A in breast cancer by simultaneous targeting of DNA and E2F1 methylation. PLoS One 2012;7:e52231.
18. Dong C, Wu Y, Yao J, Wang Y, Yu Y, Rychahou PG, *et al.* G9a interacts with Snail and is critical for Snail-mediated E-cadherin repression in human breast cancer. J Clin Invest 2012;122:1469-1486.

19. Dong C, Wu Y, Wang Y, Wang C, Kang T, Rychahou PG, *et al.* Interaction with Suv39H1 is critical for Snail-mediated E-cadherin repression in breast cancer. Oncogene 2013;32:1351-1362.
20. Schmiegel W, Roeder C, Schmielau J, Rodeck U, Kalthoff H. Tumor necrosis factor alpha induces the expression of transforming growth factor alpha and the epidermal growth factor receptor in human pancreatic cancer cells. Proc Natl Acad Sci USA 1993;90:863-867.
21. Barsyte-Lovejoy D, Li F, Oudhoff MJ, Tatlock JH, Dong A, Zeng H, et al. (R)-PFI-2 is a potent and selective inhibitor of SETD7 methyltransferase activity in cells. Proc Natl Acad Sci USA 2014; 111:12853-12858.
22. Guttilla IK, Phoenix KN, Hong X, Tirnauer JS, Claffey KP, White BA. Prolonged mammosphere culture of MCF-7 cells induces an EMT and repression of the estrogen receptor by microRNAs. Breast Cancer Res Treat 2012;132:75-85.
23. Leis O, Eguiara A, Lopez-Arribillaga E, Alberdi MJ, Hernandez-Garcia S, Elorriaga K, *et al.* Sox2 expression in breast tumours and activation in breast cancer stem cells. Oncogene 2012;31:1354-1365.
24. Nakshatri H. Radiation resistance in breast cancer: are $CD44^{+}/CD24^{-}$/proteosome $^{low}/PKH26^{+}$ cells to blame? Breast Cancer Res. 2010;12:105.
25. Mukherjee D, Zhao J. The role of chemokine receptor CXCR4 in breast cancer metastasis. Am J Cancer Res 2013;3:46-57.
26. Liu Z, Li Q, Li K, Chen L, Li W, Hou M, *et al.* Telomerase reverse transcriptase promotes epithelial-mesenchymal transition and stem cell-like traits in cancer cells. Oncogene 2013;32:4203-4213.

27. Veronesi U, Paganelli G, Viale G, Luini A, Zurrida S, Galimberti V, et al. A randomized comparison of sentinel-node biopsy with routine axillary dissection in breast cancer. N Engl J Med 2003;349:546-553.
28. Mani SA, Guo W, Liao MJ, Eaton EN, Ayyanan A, Zhou AY, *et al.* The epithelial-mesenchymal transition generates cells with properties of stem cells. Cell 2008;133:704-715.
29. Morel AP, Lièvre M, Thomas C, Hinkal G, Ansieau S, Puisieux A. Generation of breast cancer stem cells through epithelial-mesenchymal transition. PLoS One 2008;3:e2888.
30. Rhim AD1, Mirek ET, Aiello NM, Maitra A, Bailey JM, McAllister F, *et al.* EMT and dissemination precede pancreatic tumor formation. Cell 2012;148:349-361.
31. Scheel C, Weinberg RA. Phenotypic plasticity and epithelial-mesenchymal transitions in cancer and normal stem cells? Int J Cancer 2011;129:2310-2314.
32. Kalluri R, Weinberg RA. The basics of epithelial-mesenchymal transition. J Clin Invest 2009;119:1420-1428.
33. Christofori G. New signals from the invasive front. Nature 2006;441:444-450.
34. Muñoz P, Iliou MS, Esteller M. Epigenetic alterations involved in cancer stem cell reprogramming. Mol Oncol 2012;6: 620-636.
35. Engelmann D, Pützer BM. The dark side of E2F1: in transit beyond apoptosis. Cancer Res 2012;72:571-575.
36. Engelmann D, Knoll S, Ewerth D, Steder M, Stoll A, Pützer BM. Functional interplay between E2F1 and chemotherapeutic drugs defines immediate E2F1 target genes crucial for cancer cell death. Cell Mol Life Sci 2010;67:931-948.
37. Hanada N, Lo HW, Day CP, Pan Y, Nakajima Y, Hung MC. Co-regulation of B-Myb expression by E2F1 and EGF receptor. Mol Carcinog 2006; 45:10-17.

38. Tao D, Pan Y, Jiang G, Lu H, Zheng S, Lin H, et al. B-Myb regulates snail expression to promote epithelial-to-mesenchymal transition and invasion of breast cancer cell. Med Oncol 2015;32:412.
39. Yui S, Tomita K, Kudo T, Ando S, Yamazaki M. Induction of multicellular 3-D spheroids of MCF-7 breast carcinoma cells by neutrophil-derived cathepsin G and elastase. Cancer Sci. 2005;96:560-570.
40. Chaffer CL, Weinberg RA. A perspective on cancer cell metastasis. Science 2011;331:1559-1564.
41. Hirohashi S. Inactivation of the E-cadherin-mediated cell adhesion system in human cancers. Am J Pathol 1998;53:333-339.
42. Cavallaro U, Christofori G. Cell adhesion in tumor invasion and metastasis: loss of the glue is not enough. Biochim Biophys Acta 2001;1552:39-45.
43. Iglesias J, Beloqui I, Garcia-Garcia F, Leis O, Vazquez-Martin A, Eguiara A, et al. Mammosphere formation in breast carcinoma cell lines depends upon expression of E-cadherin. PLoS One 2013;8:e77281.
44. Gupta A, Deshpande CG, Badve S. Role of E-cadherins in development of lymphatic tumor emboli. Cancer 2003;97:2341-2347.
45. Jaggupilli A, Elkord E. Significance of CD44 and CD24 as cancer stem cell markers: an enduring ambiguity. Clin Dev Immunol 2012;2012:708036.
46. Geng Y, Chandrasekaran S, Hsu JW, Gidwani M, Hughes AD, King MR. Phenotypic switch in blood: effects of pro-inflammatory cytokines on breast cancer cell aggregation and adhesion. PLoS One 2013;8:e54959.
47. Harris WJ, Huang X, Lynch JT, Spencer GJ, Hitchin JR, Li Y, *et al.* The histone demethylase KDM1A sustains the oncogenic potential of MLL-AF9 leukemia stem cells. Cancer Cell 2012;21:473-487.

48. Schenk T, Chen WC, Göllner S, Howell L, Jin L, Hebestreit K, *et al.* Inhibition of the LSD1 (KDM1A) demethylase reactivates the all-trans-retinoic acid differentiation pathway in acute myeloid leukemia. Nat Med 2012;18:605-611.
49. Lim S, Janzer A, Becker A, Zimmer A, Schüle R, Buettner R, *et al.* Lysine-specific demethylase 1 (LSD1) is highly expressed in ER-negative breast cancers and a biomarker predicting aggressive biology. Carcinogenesis 2010;31:512-520.
50. Wu Y, Wang Y, Yang XH, Kang T, Zhao Y, Wang C, *et al.* The deubiquitinase USP28 stabilizes LSD1 and confers stem-cell-like traits to breast cancer cells. Cell Rep. 2013;5:224-236.
51. Chang HW, Wang HC, Chen CY, Hung TW, Hou MF, Yuan SS, et al. 5-azacytidine induces anoikis, inhibits mammosphere formation and reduces metalloproteinase 9 activity in MCF-7 human breast cancer cells. Molecules 2014;19:3149-3159.
52. Sáez-Ayala M, Montenegro MF, Sánchez-Del-Campo L, Fernández-Pérez MP, Chazarra S, Freter R, *et al.* Directed phenotype switching as an effective antimelanoma strategy. Cancer Cell 2013;24:105-119.
53. Edge SB, Compton CC. The American Joint Committee on Cancer: the 7th edition of the AJCC cancer staging manual and the future of TNM. Ann Surg Oncol 2010;17;1471-1474.
54. Singh JK, Farnie G, Bundred NJ, Simões BM, Shergill A, Landberg G, *et al.* Targeting CXCR1/2 significantly reduces breast cancer stem cell activity and increases the efficacy of inhibiting HER2 via HER2-dependent and -independent mechanisms. Clin Cancer Res 2013;19:643-656.

FIGURE LEGENDS

Figure 1. Expression of SET9 is negatively correlated with DNMT1 protein levels. (**a**) The levels of SET9 and DNMT1 mRNA in BC cell lines were analyzed by real-time RT-PCR. The values shown represent the number of copies for every 10^3 copies of β-actin. Protein expression was analyzed by WB. (**b**) The DNMT1 expression from 8 fresh-frozen human breast tumor samples was examined by WB (left panel). The right panel shows the relationship between SET9 mRNA expression and the indicated protein abundance in 36 fresh-frozen human breast tumor samples. The mRNA axis represents the number of SET9 mRNA copies for every 10^6 copies of β-actin, whereas the protein abundance axis indicates the protein expression, as estimated by integrated optical density (IOD) in WBs after normalization to the β-actin IOD. The values represent the mean from two experiments performed in triplicate (r_s, Spearman correlation coefficient). (**c**) SET9 was overexpressed or knocked down in the indicated BC cell lines and endogenous DNMT1 was analyzed by immunofluorescent staining. Cells were labeled 48 h after transfection. (**d**) SET9 controls DNMT1 protein levels but not mRNA levels. (**e**) Expression of SET9 after silencing DNMT1 or inhibiting DNMT1 with 5-Aza-dC (1 μM; 3 days), as analyzed by WB and real-time RT-PCR. In all of the experiments asterisks denote $P < 0.05$ when compared with the appropriate controls.

Figure 2. SET9 contributes to the epigenetic regulation of EMT in BC cells. (**a**) Indicated protein expression was analyzed by immunofluorescence staining in MDA-MB-231 cells transfected with control or pcDNA-SET9-WT vectors. The migratory ability was analyzed using a wound healing assay. Statistical analysis of the migration rate (MR) is indicated (mean ± SD from 5 independent experiments; $P < 0.002$). Scale bar, 100 μm. (**b**) Protein expression in MCF7 cells transfected with control or SET9-siRNA was analyzed by confocal microscopy. BC cell invasiveness was analyzed using a Boyden chamber invasion assay. (**c**) The presence of H3K4me2/3 (H3K4) and H3K9me3 (H3K9) at E-cadherin (E-Cad) and SET9 promoters in MCF7 cells transfected with control- or SET9-siRNA was analyzed by ChIP. (**d**) The association of endogenous Snail and DNMT1 at the E-cadherin promoter was analyzed by ChIP. (**e**) SET9 silencing or TNFα treatment (50 nM; 4 days) of MCF7 cells significantly increased the occupancy of both DNMT1 and Snail at the SET9 promoter, as determined by ChIP experiments. SET9 promoter methylation was examined by methylation-specific PCR

(MSP). In all of the experiments asterisks denote $P < 0.05$ when compared with the appropriate controls.

Figure 3. SET9 modulates E2F1 protein stability, which controls Snail expression and transactivation to indirectly regulate SET9 promoter activity. (**a**) Expression of SET9 is negatively correlated with E2F1 protein levels (see also Figure 1). Surgical specimens of BC were immunostained using antibodies against SET9, E2F1, and control serum (data not shown). Representative images of IHC staining from two tumor samples are shown in the right panel. (**b**) Endogenous E2F1 was analyzed by confocal microscopy under the indicated conditions. (**c**) Mutating Lys185 stabilizes E2F1 protein, when compared with E2F1-(WT) and after overexpressing each in MCF7-(SET9-positive) cells. E2F1 stabilization downregulated SET9 and activated EMT in MCF7 cells, as demonstrated by the expression levels of selected proteins after WB and confocal microscopy experiments. The presence of Snail at E-Cad and SET9 promoters in MCF7 cells transfected with E2F1 pcDNA3 vectors (control, E2F1-WT and E2F1-K185L) was analyzed by ChIP. (**d**) Effects of silencing E2F1 in MDA-MB-231 on SET9, Snail, and selected luminal and basal marker expression. The relative mRNA levels (copies for every 10^3 copies of β-actin) were determined by real-time RT-PCR (histograms), and Snail was also confirmed by conventional RT-PCR. ChIP experiments were used to assess Snail presence at the E-Cad and SET9 promoters. In all of the experiments asterisks denote $P < 0.05$ when compared to the appropriate controls.

Figure 4. The SET9 phenotype determines mammosphere formation and differentiation in MCF7 cells. (**a**) The effect of SET9 silencing or overexpression in MCF7 cells on primary mammosphere-forming efficiency (MFE). $*P < 0.005$ with respect to control cells. (**b**) SET9 silencing accelerated dedifferentiation in MCF7-derived mammospheres. Morphological changes in siSET9-MCF7 mammospheres were paralleled by a decrease in E-cadherin (red) and increase in SOX2 (green), as determined by both bright field and confocal microscopy. The number of dedifferentiated mammospheres was determined in control and siSET9-MCF7 mammosphere cultures base on cell morphology. The results (right panel) represent the mean ± SD from three experiments that were run in triplicate. (**c**) FACS analysis for CD24 and CD44 surface markers in MCF-7 and MDA-MB-231 cells growing under different conditions. (**d**) Several genes in BC cells related to identification, growth, and stem cell differentiation are presented as a heat map of selected transcripts analyzed by PCR array. Expression values were normalized over the expression of β-actin and presented as the log_{10} of relative change

compared to their expression in MCF7 cells. Genes with higher expression are depicted in red, genes with lower expression are depicted in green, and genes with no difference are depicted in black. Genes overexpressed or downregulated by a factor higher than 4-fold in siSET9-MCF7 and overSET9-MDA-MB-231 mammospheres, with respect to their corresponding parenteral cell lines, are represented in the histograms.

Figure 5. SET9 as an early prognostic marker for BC malignancy. (**a**) The left panel shows SET9 mRNA expression levels in samples from patients harboring benign tumors (n = 10) or those that showed pCR (n =37) or Non-pCR (n = 38). Values are normalized to β-actin and represent the number of copies for every 10^6 copies of β-actin. The right panel shows the sensitivity and specificity of SET9 by ROC analysis. All BC patients with a follow-up schedule lasting at least 12.0 months (n = 75) showed an AUC of 0.93. At 5,336 copies of SET9 mRNA per 10^6 copies of β-actin (the same cutoff used in the test cohort), the sensitivity and specificity were 0.92 and 0.77, respectively. (**b, c**) Kaplan-Meier estimated overall survival (OS) and disease-free survival (DFS) rates according SET9 mRNA expression. Tumors (n = 75) were split into higher or lower values than the cutoff level determined by ROC analysis. (**d**) Kaplan-Meier estimated DFS rates in ERα tumors (n = 52) were calculated as previously described. (**e**) Representative IHC staining for SET9 in human BC tumors. (**f**) CRIF-values calculated in FFPE samples of BC using IHC to detect SET9 protein (see Supplementary Table S1). The dashed red line indicates the cutoff used in the test cohort. By ROC analysis the optimal cutoff level was CRIF = 46,048, which gave a specificity of 0.86 and a sensitivity level of 0.84. The black asterisks indicate deceased patients who were not diagnosed with local recurrence (LR) or distant metastasis (DM), and the red asterisks indicate patients diagnosed with LR but not with DM.

Figure 6. Schematic showing the negative feedback loop between SET9 and DNMT1 and the reciprocal regulation of SET9 and E2F1. By controlling the stability of E2F1 and DNMT1, the tumor suppressor SET9 is involved in the epigenetic regulation of EMT in BC cells.

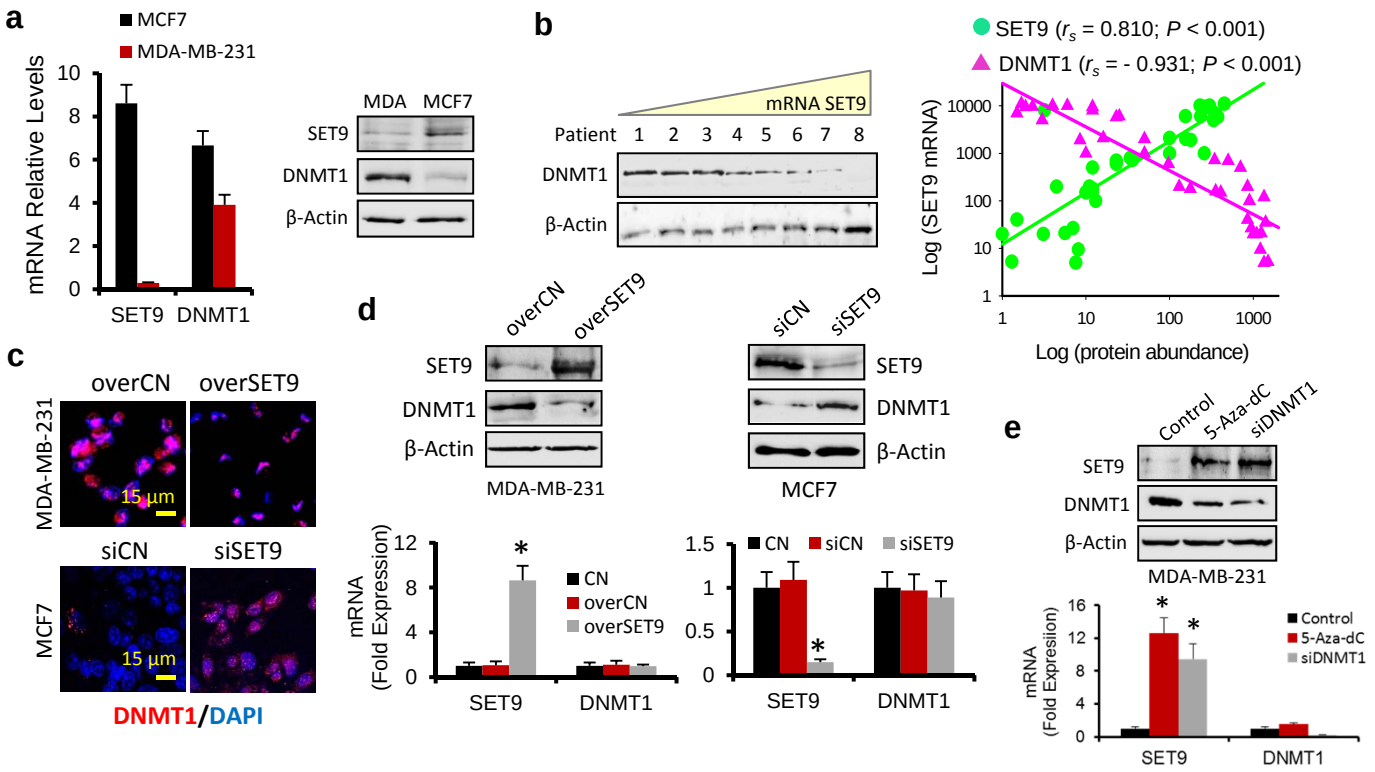

Fig. 1. Montenegro et al.

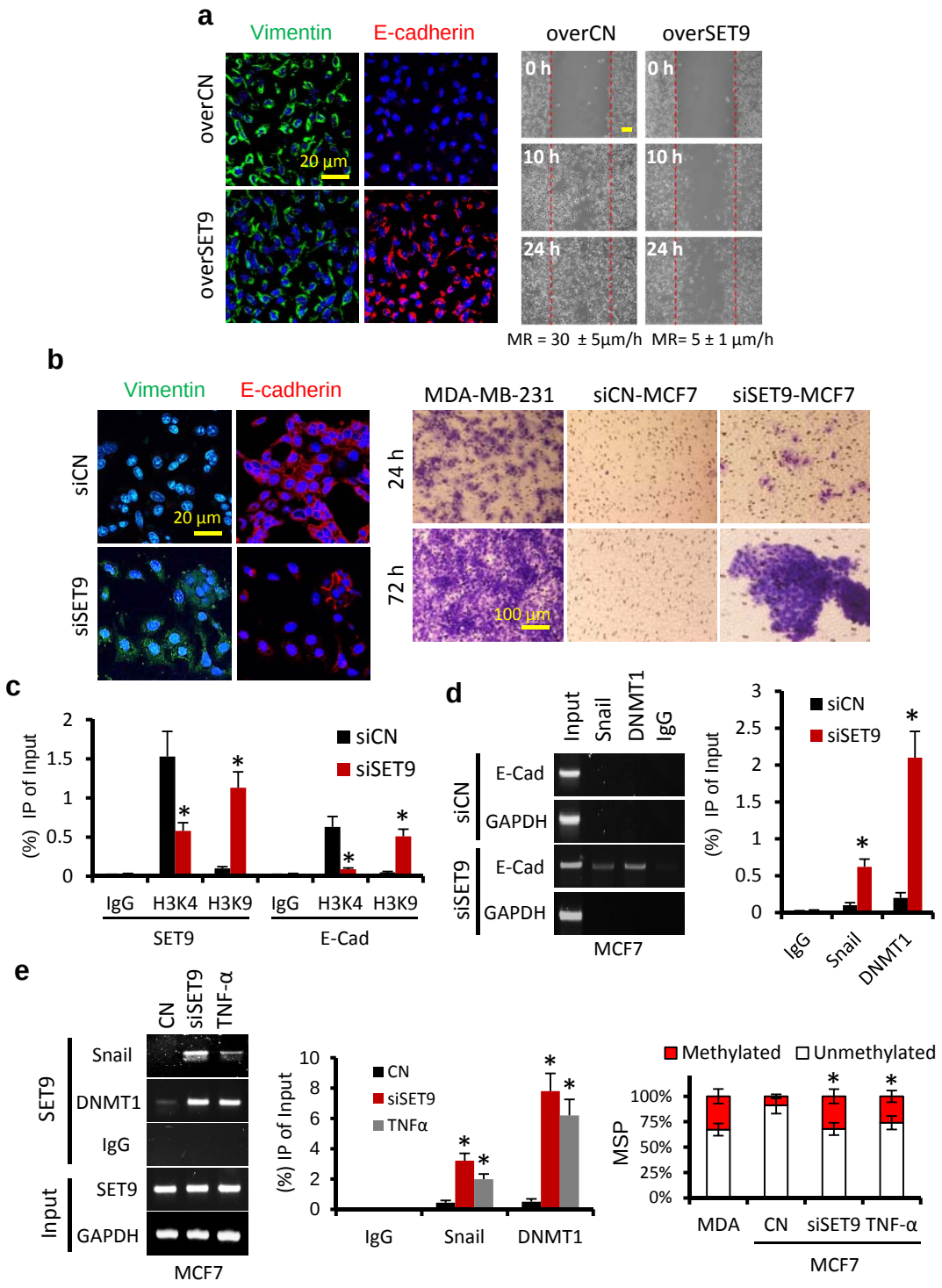

Fig. 2. Montenegro et al.

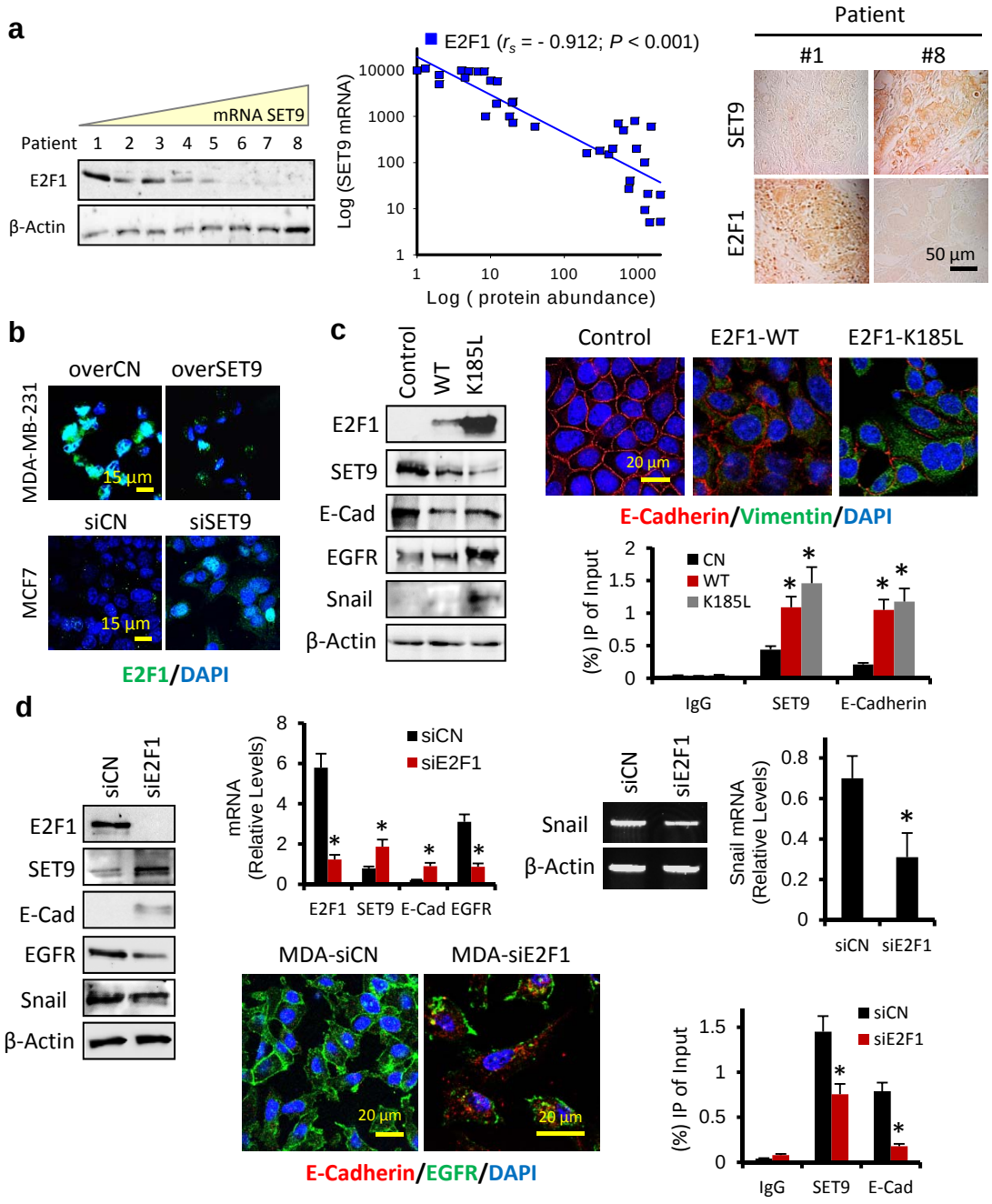

Fig. 3. Montenegro et al.

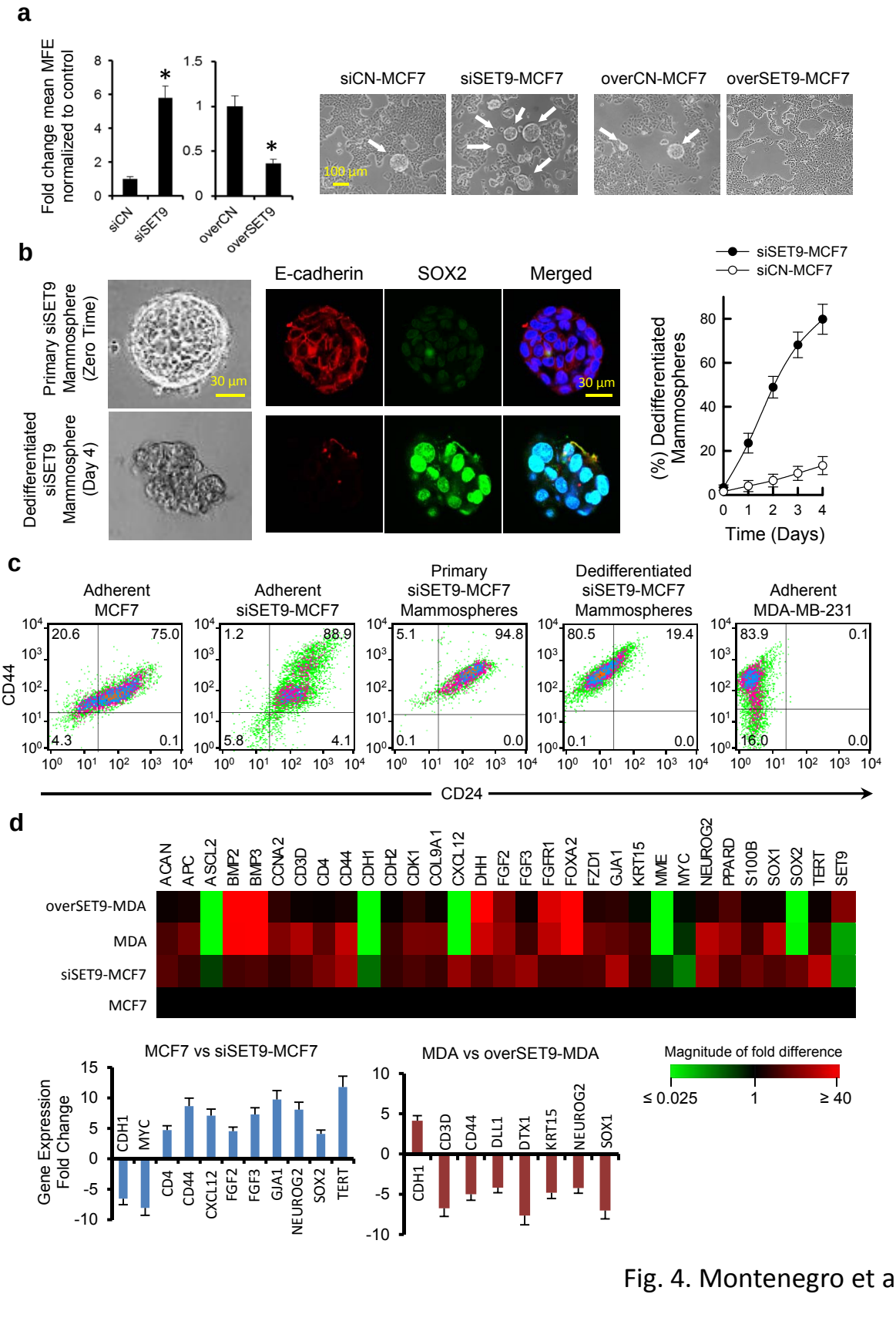

Fig. 4. Montenegro et al.

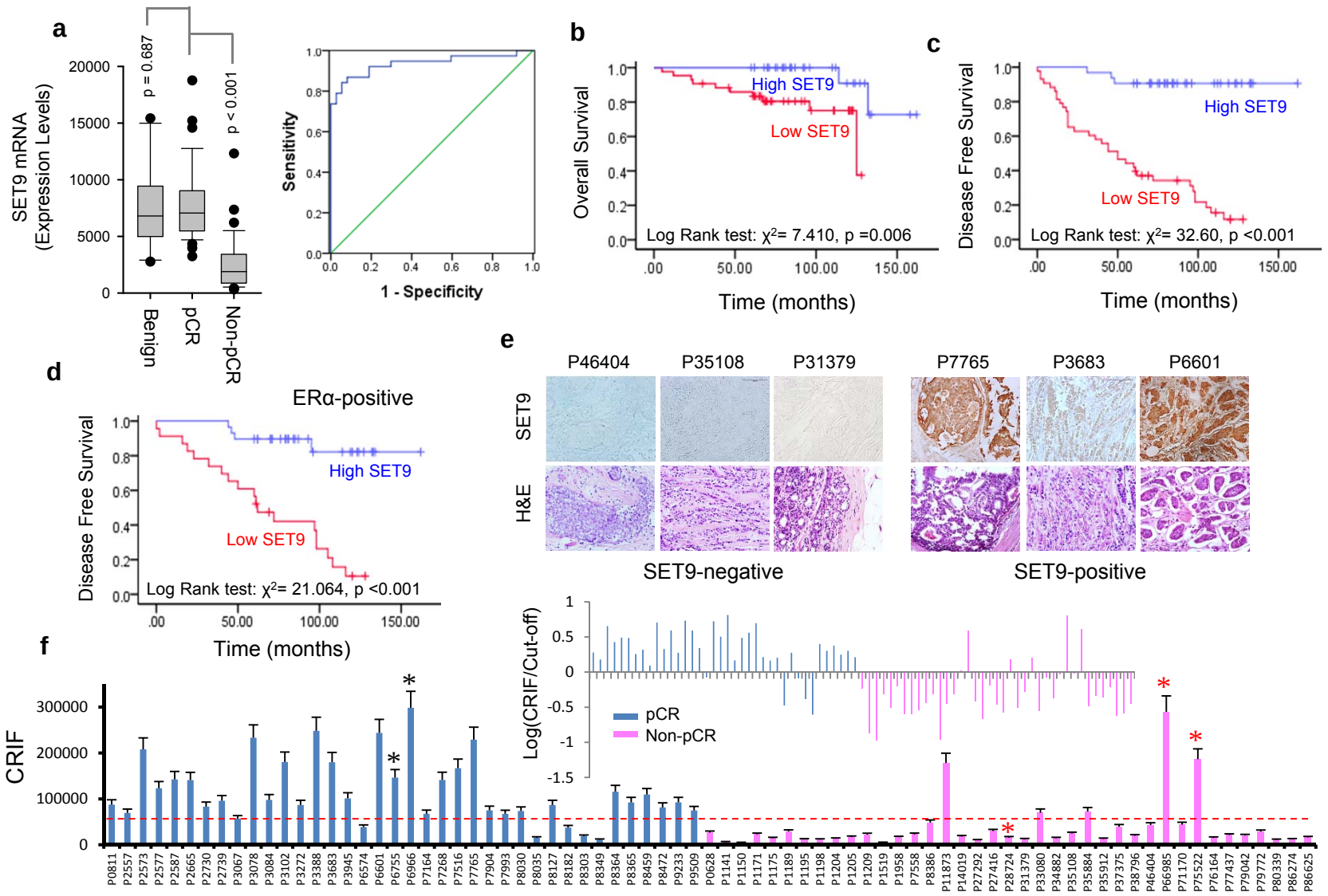

Figure 5. Montenegro et al.

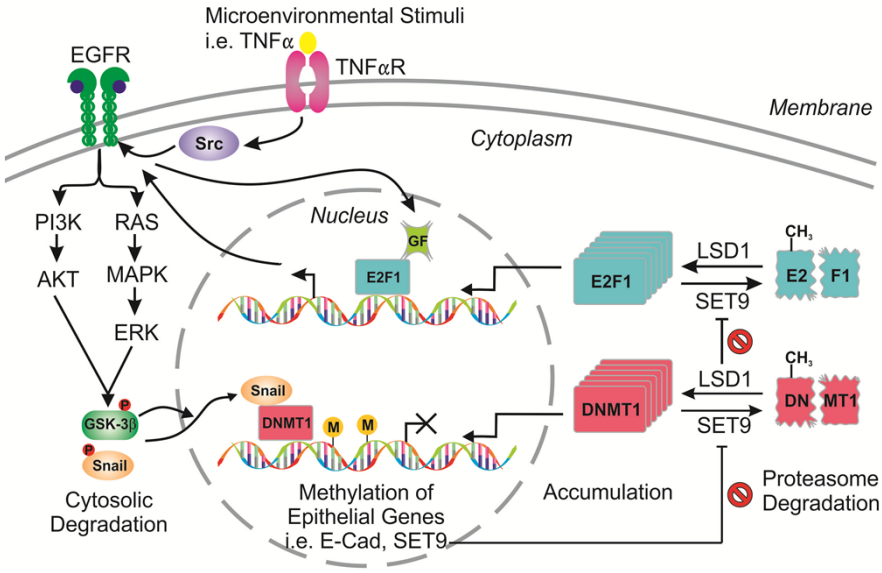

Fig. 6. Montenegro et al.